



ALMA MATER STUDIORUM  
UNIVERSITÀ DI BOLOGNA

ARCHIVIO ISTITUZIONALE  
DELLA RICERCA

## Alma Mater Studiorum Università di Bologna Archivio istituzionale della ricerca

Recycling shredded waste cigarette butts as stabilising fibres in stone mastic asphalt concretes

This is the final peer-reviewed author's accepted manuscript (postprint) of the following publication:

*Published Version:*

Guo, Y., Tataranni, P., Tarsi, G., Sangiorgi, C. (2023). Recycling shredded waste cigarette butts as stabilising fibres in stone mastic asphalt concretes. *INTERNATIONAL JOURNAL OF PAVEMENT ENGINEERING*, 24(1), 1-13 [10.1080/10298436.2023.2229477].

*Availability:*

This version is available at: <https://hdl.handle.net/11585/933616> since: 2023-07-05

*Published:*

DOI: <http://doi.org/10.1080/10298436.2023.2229477>

*Terms of use:*

Some rights reserved. The terms and conditions for the reuse of this version of the manuscript are specified in the publishing policy. For all terms of use and more information see the publisher's website.

This item was downloaded from IRIS Università di Bologna (<https://cris.unibo.it/>).  
When citing, please refer to the published version.

(Article begins on next page)

1 **Recycling Shredded Waste Cigarette Butts as Stabilising Fibres in Stone**

2 **Mastic Asphalt Concretes**

3 Yunfei Guo<sup>a\*</sup>, Piergiorgio Tataranni<sup>a</sup>, Giulia Tarsi<sup>a</sup>, Cesare Sangiorgi<sup>a</sup>

4 *<sup>a</sup>Department of Civil, Chemical, Environmental and Materials Engineering, University*  
5 *of Bologna, Via Terracini 28, 40131 Bologna, Italy*

6 \*Corresponding author: Yunfei Guo

7 Address: Via Terracini 28, 40131, Bologna, Italy

8 Phone: (+39) 3242803059

9 Email: [yunfei.guo2@unibo.it](mailto:yunfei.guo2@unibo.it)

1 **Recycling Shredded Waste Cigarette Butts as Stabilising Fibres in Stone**  
2 **Mastic Asphalt Concretes**

3 **ABSTRACT**

4 Considering the global burden of cigarette consumption, the disposal of  
5 cigarette butts has become an inevitable issue. Compared to traditional  
6 disposal methods, such as landfilling or incinerating, the recycling of  
7 these wastes is clearly an eco-friendlier solution. In this research, waste  
8 electronic cigarette butts (E-CBs) were collected and recycled in  
9 bituminous mixtures, aiming to increase the use of sustainable road  
10 construction materials. The objective of this research is to explore the  
11 possibility of using waste E-CBs as an alternative stabilising fibre in  
12 asphalt mixtures. To this end, shredded waste E-CBs were incorporated in  
13 Stone Mastic Asphalt (SMA) and compared with the conventional  
14 cellulose fibres. Furthermore, to investigate the effects of powders (below  
15 0.063 mm) from the waste E-CBs on the rheological properties of bitumen,  
16 tests were conducted on base SBS-modified bitumen and its mastics.  
17 Results show that the waste powder was unfavourable to the thermal  
18 susceptibility of the resulting binder. SMA samples with shredded E-CBs  
19 were also characterised through physical and mechanical tests and  
20 compared to the reference mixture using cellulose fibres. It was concluded  
21 that using waste E-CBs in SMA can be considered a promising alternative  
22 for replacing cellulose fibres and avoiding the disposal of cigarette butts.

23 **Keywords:** waste cigarette butts; stabilizing fibres; SMA mixtures;  
24 rheology; mechanical properties

## 1 **1 Introduction**

2 In recent years, waste or recycled materials have been increasingly used in road  
3 construction for the sake of environmental protection and sustainable development.  
4 Apart from the reclaimed asphalt pavement (RAP) materials that were effectively  
5 recycled since the 1970s (Willis and Yin 2022), the possibilities of using other waste  
6 materials such as plastic waste, crumb rubber, waste cooking oil, fibre-based materials  
7 (coconut, sisal, cellulose, glass, polyester, etc.) and steel slag have been explored by  
8 researchers (Rahman *et al.* 2020a, Victory 2022). The proper application of waste  
9 materials into pavements can be an environmental-friendly solution to promote the  
10 recycling of valuable products while solving disposal issues. It helps to reduce the use  
11 of landfill sites, non-renewable resources and unnecessary pollution caused by  
12 incineration, and manufacturing costs for raw materials.

13 The increasing production and extensive use of traditional cigarettes and  
14 electronic cigarettes (e-cigarettes) made cigarette butts and filters (CBs, CFs) one of the  
15 most littered garbage items and a very common source of pollution worldwide. A  
16 dramatic increase in the use of e-cigarettes has been recorded among young users  
17 (Eurobarometer 2015, Cullen *et al.* 2019, Giovacchini *et al.* 2022). A large amount of  
18 global cigarette consumption not only brings serious health problems to humans, but  
19 the disposal of CBs is also a critical issue. According to a recent report, nearly 1.2  
20 million tons of CBs are produced every year (Mohajerani *et al.* 2016). Especially, the  
21 CBs discarded on beaches worldwide made up the largest proportion of garbage

1 annually (Ocean Conservancy, 2021), and up to 40% of the whole marine debris  
2 collected (Hidalgo-Ruz *et al.* 2018). CBs are considered as one unique waste due to  
3 their double contamination, physical and chemical (Dobaradaran *et al.* 2021). Physical  
4 pollution is because CBs or some parts of them can be the food source for marine  
5 animals (Compa *et al.* 2018), and they are also a source of microplastic fibres that are  
6 non-biodegradable (Gerritse *et al.* 2020). In chemical terms, above 7000 chemicals  
7 from CBs can leach into the planet, many of which are detrimental to living organisms  
8 and ecosystems (Ariza *et al.* 2008, Roder Green *et al.* 2014, Cardoso *et al.* 2018,  
9 Dobaradaran *et al.* 2022, Soleimani *et al.* 2022). One issue that needs to be addressed  
10 is the random littering of CBs in the environment brought on by users' poor awareness.  
11 Additionally, more sustainable alternatives should be developed to replace the current  
12 disposal methods (landfilling or burning) (Tataranni and Sangiorgi 2021). Recycling  
13 CBs is an effective method to reduce the harmful effect on the environment and lessen  
14 disposal issues.

15         One bio-based component of CB, namely cellulose acetate fibre, is a renewable  
16 synthetic polymer. Different recycling methods for CBs have been explored by  
17 researchers. The application of reusing CBs has been involved in varying industrial  
18 fields, i.e. construction and infrastructure, energy and environment, medical and  
19 chemical industries (Conradi and Sánchez-Moyano 2022). Specifically, the recycling  
20 of CBs in asphalt pavements has been investigated in recent years. In the research  
21 conducted by Mohajerani *et al.* (2017), CBs encapsulated with bitumen or paraffin were

1 added into Dense Grade Asphalt (DGA) mix and compared to the asphalt concrete  
2 samples without CBs. The results proved that 10 kg/m<sup>3</sup> or 15 kg/m<sup>3</sup> bitumen  
3 encapsulated CBs can be recycled in DGA mixtures, showing acceptable volumetric  
4 and mechanical properties (bulk density, air-void contents, flow, stability and resilient  
5 modulus). Rahman and Mohajerani (2020) also investigated bitumen and wax  
6 encapsulated CBs in Stone Mastic Asphalt (SMA). It was found that stability and rutting  
7 resistance can be improved with the use of encapsulated CBs. In another study by  
8 Rahman et al. (2020b), CBs were recycled as fibres in bitumen. A series of processing  
9 procedures were performed before blending them with bitumen, which includes drying,  
10 removing the excess tobacco and shredding them into ground fibres. According to the  
11 results, the incorporation of CBs significantly improved the physical and rheological  
12 properties of bitumen. In another research by Tataranni and Sangiorgi (2021), new  
13 electronic cigarette filters (E-CFs) after being shredded into particles up to 10 mm were  
14 added into SMA and compared with traditional cellulose fibres. Testing results proved  
15 that shredded CFs can be successfully used as stabilising fibres and a sustainable  
16 alternative to cellulose fibres for SMA mixes.

17         The above research studies concerning the use of CBs or CFs in bitumen or  
18 bituminous mixtures confirmed the recyclability of this type of waste materials and  
19 provided a good solution to their disposal. In terms of the waste E-CBs, one of the  
20 rapidly growing waste sources in the world, their reuse is worthy of further  
21 investigation. Although the research by Tataranni and Sangiorgi (2021) explored the

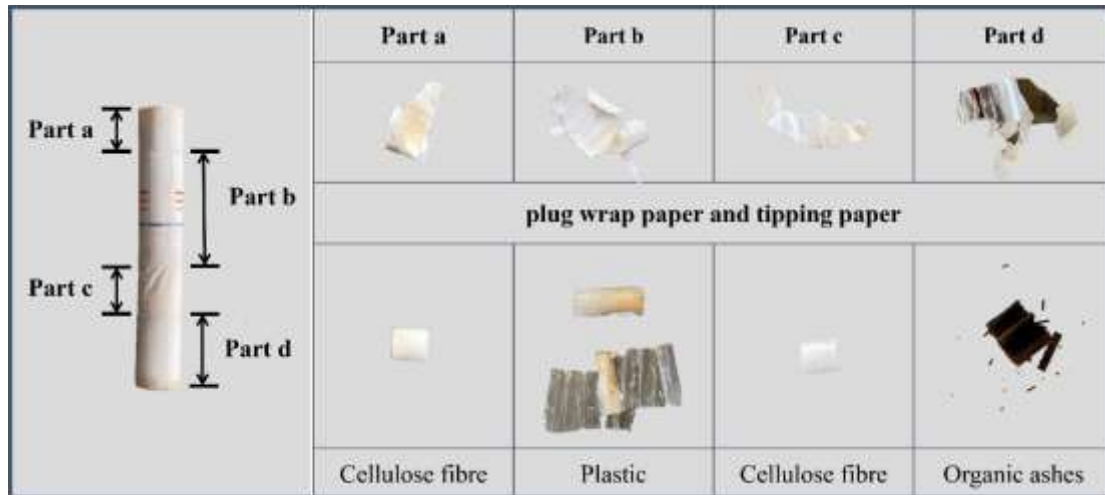
1 possibility of recycling new E-CFs without tobacco in SMA, the recyclability of waste  
2 E-CBs that were littered by smokers after consuming cigarettes needs to be further  
3 investigated. To verify the possibility of recycling waste E-CBs in asphalt mixtures,  
4 SMA mixtures with the addition of shredded waste E-CBs as stabilising fibres were  
5 manufactured and analysed in comparison with a reference mix with traditional  
6 cellulose fibres. In addition, the effects of powders (below 0.063 mm) from the waste  
7 E-CBs on the rheological properties of bitumen were investigated. The objective of this  
8 research is to evaluate the possibility of recycling waste E-CBs in asphalt paving  
9 materials and so define a possible environmental-friendly alternative to their disposal.

## 10 **2 Materials and Methods**

### 11 *2.1 Waste-based fibres from electronic cigarette butts and cellulose fibres*

12 Waste electronic cigarette butts (E-CBs) were collected and used as the substitution for  
13 traditional stabilizing fibres in this research. As shown in Figure 1, each waste E-CB  
14 can be separated and divided into 4 main parts. The components of the waste CB are  
15 cellulose fibres, plastic, organic ashes, with traces of plug wrap paper and tipping paper.

16 The length of each part and the weight percentage of each component are listed in Table  
17 1. Before the addition of waste E-CB into asphalt mixtures, they were shredded with  
18 the use of a mechanical shredder. Particles with a size below 10 mm were obtained  
19 (Figure 2 (a)) and have been used as waste fibres in this research.

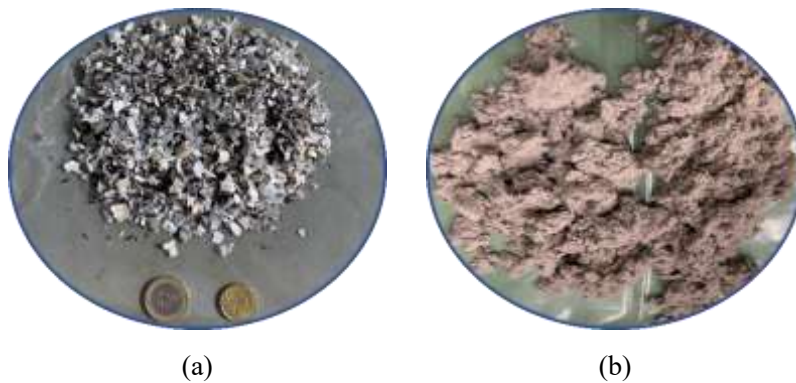


1  
2 **Figure 1. Four parts of a single electronic cigarette butt**

3 **Table 1. Length of each part and weight percentage of each component in one E-CB**

Name	Length (mm)	Weight (g)	Weight percentage (%)
One waste E-CB	44.96	2.25	100
Part a-cellulose fibre	7.15	0.10	4
Part b-plastic	17.67	0.76	34
Part c-cellulose fibre	8.04	0.19	8
Part d-organic ashes	12.17	0.71	32
remaining material		0.49	22

4 Note: the remaining material includes the paper and the loss when calculating the weight percentage  
5 of each material



6 **Figure 2. (a) Shredded waste E-CBs (below 10 mm) and (b) cellulose fibres**

7 One of the traditional stabilising fibres, the cellulose fibres shown in Figure 2  
8 (b), was used as the reference. The technical properties of cellulose fibres are listed in  
9 Table 2.

10

1 **Table 2. Technical properties of cellulose fibres**

Technical properties of cellulose fibres	Value
Length of average fibres ( $\mu\text{m}$ )	200-1100
Diameter of average fibres ( $\mu\text{m}$ )	25-45
Melting point ( $^{\circ}\text{C}$ )	>230
Water solubility (%)	0.450-0.500 $\text{kg}/\text{m}^3$

2 **2.2 Polymer modified bitumen (PmB)**

3 Polymer modified bitumen (PmB) with the high resistance to deformation that is  
 4 usually used for roads under heavy traffic, was selected to produce asphalt mixtures in  
 5 this study. The basic properties of the SBS-modified bitumen are given in Table 3.

6 **Table 3. Basic properties of the PmB**

Property	Value	Standard
Penetration (dmm, @ 25 $^{\circ}\text{C}$ )	45-80	(EN 1426 2015)
Softening Point ( $^{\circ}\text{C}$ )	$\geq 70$	(EN 1427 2015)
Dynamic viscosity ( $\text{Pa}\cdot\text{s}$ , @ 160 $^{\circ}\text{C}$ )	< 0.8	(EN 13702-1 2003)
Elastic recovery (% , @ 25 $^{\circ}\text{C}$ )	$\geq 80$	(EN 13398 2017)
Storage stability-softening point ( $^{\circ}\text{C}$ )	$\leq 5$	(EN 13399 2017)

7 **2.3 Mastic samples preparation**

8 To investigate the effects of powder with filler size from the shredded waste E-CBs on  
 9 the rheological properties of bitumen, two mastic samples were prepared. One is given  
 10 by the mix of PmB and limestone filler, namely PmB+F. The other, called PmB+F+P,  
 11 is the mix of PmB, limestone filler and waste powder (materials from shredded E-CBs  
 12 passing the 0.063 mm sieve). The ratio of each material in the mastic was defined in  
 13 accordance with the weight percentage of the corresponding material in the asphalt  
 14 mixture. During the preparation of the mastic PmB+F, PmB was preheated at 180  $^{\circ}\text{C}$   
 15 for two hours and then mixed with fillers at 170-180  $^{\circ}\text{C}$  for 5 min with a speed of 500

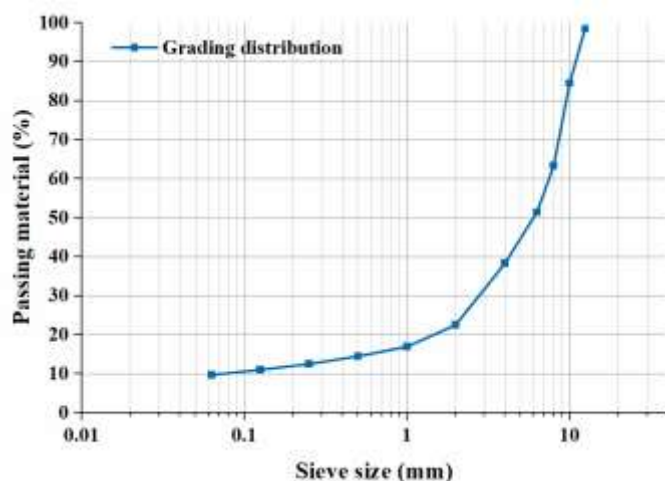
1 rpm. Then the blend was heated in the oven for 30 min. For the preparation of PmB+F+P,  
2 powders were added into PmB before adding the fillers. The following blending  
3 procedures were the same.

#### 4 ***2.4 SMA mixtures preparation***

5 SMA mixture is a gap-graded asphalt concrete requiring high-quality aggregates, in  
6 which the higher percentage of air voids if compared to a traditional dense mix, is filled  
7 with modified bitumen, stabilising fibres and fine aggregates (Vázquez *et al.* 2019). As  
8 one of the mixed design methodologies, SMA is highly recommended in high-traffic  
9 roads due to its excellent performance in rutting resistance, low-temperature cracking  
10 resistance, skid resistance, good durability and low noise. In this study, PmB, porphyry  
11 aggregates and limestone filler were selected to produce SMA mixtures. Following the  
12 previous research studies (Eskandarsefat *et al.* 2019, Tataranni and Sangiorgi 2021), the  
13 optimum bitumen content and filler content were 6% and 10% on the weight of  
14 aggregates, respectively. According to the local standard in the District of Bologna  
15 (Italy) (Capitolato Speciale d'Appalto. Comune di Bologna. 2018), the grading  
16 distribution is displayed in Table 4 and Figure 3.

1 **Table 4. Aggregate gradation in SMA mix design**

Sieve (mm)	Retained materials (%)	Passing materials (%)
14	0.00	100.00
12	1.56	98.44
10	13.98	84.45
8	21.17	63.28
6.3	11.86	51.43
4	13.02	38.41
2	15.79	22.62
1	5.65	16.97
0.5	2.49	14.48
0.25	1.93	12.55
0.125	1.54	11.01
0.063	1.22	9.79
< 0.063	9.79	-



2

3 **Figure 3. SMA grading curves**

4 During the mixture production, the experimental and traditional stabilising  
 5 fibres were added into SMA mixes producing two types of asphalt concrete. Before  
 6 using the shredded waste E-CBs as stabilising fibres in SMA (SMA-W), drain-down  
 7 tests (ASTM D6390—11 2017) were performed to determine their optimal dosage. The  
 8 other SMA with traditional cellulose fibres was selected as the reference (SMA-R).  
 9 Cellulose fibres at a ratio of 0.3% were adopted when preparing the reference mix

1 (Tataranni and Sangiorgi 2021).

## 2 ***2.5 Experimental programme***

### 3 *2.5.1 Penetration, softening point and rheological tests*

4 The basic properties of the two mastic samples and the base PmB were tested through  
5 penetration (EN 1426 2015) and softening point (EN 1427 2015) tests. The consistency  
6 of bituminous binders or mastics can be measured through the penetration value at the  
7 temperature of 25 °C. The softening point is used to assess the high temperature  
8 susceptibility of testing samples. Due to the use of PmB in this research, glycerine was  
9 used as the liquid bath.

10 Rheological properties of base modified bitumen and mastics were evaluated using a  
11 Dynamic Shear Rheometer (DSR, Anton Paar MCR 302, Austria). The rheological  
12 behaviours of the modified bitumen and the two mastics over a wide range of  
13 temperatures and frequencies were investigated through Frequency Sweep (FS) test  
14 according to the standard EN 14770 (2012). The Amplitude Sweep (AS) test was  
15 preliminarily conducted to define the linear visco-elastic (LVE) range of the three  
16 testing samples and determine the strain level of FS tests. In the AS test, samples were  
17 tested under the constant frequency of 1.59 Hz at a test temperature of 10 °C, while the  
18 range of strain level was from 0.1% to 10%. Subsequently, FS tests were carried out on  
19 the three different bituminous materials. During the FS test, each sample was subjected  
20 to an oscillatory shear stress applying a constant strain level of 0.1% at varying  
21 frequencies from 0.1 to 10 Hz, and the load was replicated at six test temperatures (10,

1 20, 30, 40, 50 and 60 °C). According to the standard ASTM D7405 (2015), the Multiple  
2 Stress Creep and Recovery (MSCR) test can be carried out to evaluate the rutting  
3 resistance of the modified bitumen and mastics. Non-recoverable creep compliance ( $J_{nr}$ )  
4 and percentage recovery (R%) are the two critical parameters obtained from MSCR  
5 tests, representing the resistance to permanent deformation and the elasticity of  
6 bituminous materials, respectively. PmB and two mastics in an unaged state were tested  
7 at 60 °C with two different stress levels (0.1 kPa and 3.2 kPa). During the test, twenty  
8 cycles at 0.1 kPa are conducted followed by 10 cycles at 3.2 kPa. Each cycle contains  
9 1 second for creep loading and 9 seconds for recovery.

#### 10 *2.5.2 Drain-down tests*

11 In this research, shredded E-CBs at the ratio of 0.3% and 0.4% on the weight of  
12 aggregates were introduced in the mixtures prepared for drain-down tests (ASTM  
13 D6390—11 2017). In this test, the mass of drained materials from a loose asphalt  
14 mixture prepared at the in-plant production temperature was measured and then the  
15 percentage of drained materials can be calculated. According to the absorption  
16 properties of shredded E-CBs, the optimum content of these experimental fibres was  
17 defined.

#### 18 *2.5.3 Physical and mechanical tests*

19 After defining the correct dosage of shredded E-CBs, the two SMA specimens with a  
20 diameter of 100 mm (SMA-W and SMA-R) were manufactured using a Gyrotory  
21 Compactor (EN 12697-31 2019). Three samples for each SMA were prepared for

1 characterising their volumetric properties. Air-voids (AV) contents at 10, 100 and 180  
2 gyrations were calculated based on the data collected from the gyratory compactor.  
3 Furthermore, the gyratory compaction curves were analysed to assess the workability  
4 and compactability of the mixtures.

5 With regard to the mechanical properties, the effects given by the substitution  
6 of cellulose fibres with shredded E-CBs were assessed via a series of standard  
7 laboratory tests. SGC samples compacted with 100 gyrations were prepared for the  
8 mechanical tests. Following the standard EN 12697-23 (2017), Indirect Tensile  
9 Strength (ITS) tests were used to evaluate the cohesion properties of SGC samples with  
10 height ranging from 35mm to 75mm at 25 °C. After placing the cylindrical specimen  
11 in the testing machine between the loading strips, the compressive loading was applied  
12 to the specimen in the diametrical direction at a constant displacement rate of  $50 \pm 2$ mm  
13 until it breaks. The peak load can be recorded subsequently. The ITS (kPa) of the test  
14 specimen can be calculated according to the following equation:

$$ITS = \frac{2P}{\pi DH} \cdot 1000 \quad (1)$$

15 where P is the peak load (N), D and H are the diameter and height of the specimen (mm).  
16 Three replicate specimens were prepared for each mixture and for each test.

17 Indirect Tensile Stiffness Modulus (ITSM) values at three test temperatures  
18 (10°C, 20°C, and 30°C) were evaluated to analyse the stiffness and thermal  
19 susceptibility of specimens (EN 12697-26: 2018). Following the standard, the height of  
20 specimen is from 40mm to  $60 \pm 2$ mm for the maximum grain size  $\leq 16$ mm. Before

1 carrying out the stiffness modulus tests, the testing sample was placed in the  
2 temperature-controlled chamber at the testing temperature for at least four hours. The  
3 Nottingham Asphalt Tester (NAT) was used to perform this non-destructive test. During  
4 the test, an impulsive load was applied with a rise time of 124 ms to achieve the target  
5 horizontal deformation of 5  $\mu\text{m}$ . The following equation was used to obtain the stiffness  
6 modulus (MPa):

$$ITSM = \frac{F}{(zh)} \cdot (v + 0.27) \quad (2)$$

7 where F is the maximum vertical load (N),  $v$  is the Poisson's ratio, z is the amplitude  
8 of the horizontal deformation and h is the height of the specimen.

9         The water susceptibility of the two different asphalt mixtures was analysed by  
10 comparing the ITS ratio (ITSR) following the standard EN 12697-12 (2018). The  
11 testing sample was immersed in the water bath at 40 °C for 72 hours before running the  
12 ITS test. The ITSR is the ratio of samples conditioned in wet and dry mode.  
13 Furthermore, the resistance to permanent deformation of SGC specimens with a height  
14 of  $60 \pm 2\text{mm}$  under the loading condition at 40 °C was measured using the Repeated  
15 Load Axial Test (RLAT) method. Following the standard EN 12697-25 (2020), a  
16 uniaxial test configuration was adopted in this research. For each mixture, three  
17 replicate specimens were prepared.

## 18 **3 Results and discussion**

### 19 ***3.1 Drain-down values of the shredded E-CBs***

20 One of the major issues of the application of SMA with high content bitumen is the

1 drain-down, which is the separation of bitumen and mastic materials from asphalt  
 2 mixtures at high temperature (Brown *et al.* 1997). Adding stabilising agents like  
 3 cellulose and mineral fibres can alleviate the drain-down problem in SMA. The correct  
 4 dosage of the stabilising fibres is based on the bitumen absorption properties of the  
 5 material used. Two dosages of shredded E-CBs were utilised to evaluate the bitumen  
 6 absorption properties of the experimental fibres. As shown in Table 5, the average drain-  
 7 down values of 0.3% and 0.4% shredded E-CBs remain at a similar level, which is less  
 8 than 0.2%. These results reached the acceptable level of the drain down value that  
 9 should be below 0.3%, as suggested by AASHTO T305 (2012). To achieve the  
 10 recycling of a higher amount of waste materials, 0.4% was selected as the optimum  
 11 dosage of shredded E-CBs in SMA.

12 **Table 5. Drain-down values of SMA-W mixes with different content of shredded E-CBs**

Content of the shredded E-CBs	Drain-down (%)
0.3%	0.12 ( $\pm 0.02$ )
0.4%	0.14 ( $\pm 0.01$ )

13 **3.2 Rheological properties of bitumen and mastics**

14 Regarding the preparation of the two mastic samples, the ratio of each material was in  
 15 line with their ratios in the SMA. According to the sieving results of shredded E-CBs,  
 16 the average percentage of powders with a size smaller than 0.063 mm was 0.68%. Based  
 17 on the contents of bitumen, fibres and fillers in the SMAs (shown in Table 6), already  
 18 introduced in the previous paragraphs, the ratio of each material in the mastic was  
 19 defined. For the sample PmB+F, PmB and fillers were blended at a mass ratio of 6:10.

1 To produce PmB+F+P mastic, the mass ratio of PmB, fillers and powders was  
 2 6:10:(0.4×0.68%). Table 7 clearly presents the weight percentage of each component in  
 3 the two mastics.

4 **Table 6. Weight percentages of bitumen, fibres and fillers in the SMA-W (on the weight of**  
 5 **aggregates)**

Composition	Bitumen	Fibres (shredded E-CBs)	fillers
Weight percentages (%)	6%	0.4%	10%

6 **Table 7. Weight percentage of each material in the two mastics**

Mastics	Components in the mastic and their weight percentages
PmB+F	37.50% PmB + 62.50% fillers
PmB+F+P	37.49% PmB + 62.49% fillers + 0.02% powders

7 *3.2.1 Penetration and softening point*

8 The penetration results tested at 25 °C and softening points of base PmB and the two  
 9 mastics are listed in Table 8. As expected, a marked decrease in penetration values was  
 10 recorded by the incorporation of filler particles regardless of its type. The penetration  
 11 values of the two mastics were less than half that of PmB. It reveals that the addition of  
 12 fillers led to a significant increase in the consistency of modified bitumen. No striking  
 13 change was found after the introduction of the waste powder coming from E-CB's  
 14 shredding. Regarding the softening points, the effect of adding filler and powder was  
 15 noticeable. The mastic with only limestone filler showed the highest softening point  
 16 value, followed by the mastic with limestone filler and waste powder, then PmB. It  
 17 indicates that the filler improved bitumen's resistance to high temperature deformation,  
 18 while the inclusion of powders was unfavourable to this improvement.

19

1 **Table 8. Penetration and softening point results**

Samples	Penetration (0.1mm, @25 °C)	Softening point (°C)
PmB	49.0 (±1.8)	92.5 (±0.1)
PmB+F	21.9 (±0.6)	103.8 (±0.7)
PmB+F+P	22.4 (±0.9)	96.7 (±0.8)

2 *3.2.2 Rheological behaviour from Frequency Sweep tests*

3 The LVE ranges of PmB and two mastic samples were identified using AS tests. In this  
 4 study, the LVE limit was defined as 95% of the initial storage modulus value. The LVE  
 5 range of bituminous materials at higher temperatures is included in the range of the  
 6 same sample tested at a lower temperature. Therefore, the LVE range of the PmB and  
 7 two mastic samples at 10 °C, which is the most restrictive LVE range, is listed in Table  
 8 9. It is clear that PmB had a wider LVE domain than the other two mastic samples.  
 9 According to the data from Table 9, 0.1% was selected as the shear strain level for  
 10 performing FS tests.

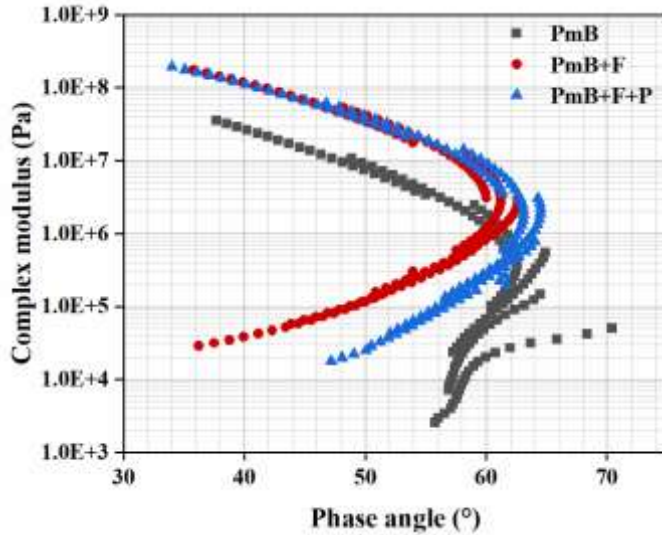
11 **Table 9. LVE ( $\gamma_{LVE}$ ) range of PmB and two mastic samples at 10 °C**

Samples	$\gamma_{LVE}$ @10 °C (%)
PmB	1.580
PmB+F	0.126
PmB+F+P	0.129

12 *3.2.2.1 Black diagram and master curves*

13 According to the data collected from the FS tests, the Black diagram displaying the  
 14 curves of complex modulus ( $G^*$ ) versus phase angle ( $\delta$ ) of all tested materials is  
 15 presented in Figure 4. Using the Black diagram is an effective method for evaluating  
 16 the effects of modifiers or fillers on the rheological behaviour of conventional  
 17 penetration grade bitumens. Unlike the conventional bitumen displaying a smooth

1 Black diagram in which the complex modulus decreased while the phase angle  
2 increased (Airey 2002), PmB used in this study showed an evident plateau region when  
3 phase angle values reached around 65°. The difference between PmB and mastic  
4 samples is visible in Figure 4. At lower temperatures (10 and 20 °C), the mastic samples  
5 showed higher complex modulus than PmB. This implies that the addition of fillers led  
6 to an increase in the stiffness of bitumen. At high temperatures (50 and 60 °C), Black  
7 diagram curves of mastic samples shifted towards a lower phase angle. Specifically,  
8 PmB+F and PmB+F+P showed higher complex modulus and decreased phase angle  
9 values compared to PmB. Therefore, the rheological changes caused by adding fillers  
10 can be recorded as the increase in stiffness and the higher contribution of the elastic  
11 behaviour. Unlike the similar Black diagram curves of two mastic samples tested at  
12 lower temperatures, the difference between them under the higher-temperature  
13 condition became significant. At high test temperature, the behaviour of filler particles  
14 become predominant on that of the bituminous matrix. At 50 and 60 °C, the presence  
15 and type of waste powder resulted in a shifting of the raw rheological data towards  
16 higher phase angle values. This means that the mastic with only limestone filler was  
17 more elastic than the mastic containing the same filler and the additional powder from  
18 shredded E-CBs. Some constituents of waste powder, including organic ashes, from E-  
19 CBs may interact in the bituminous matrix leading to a softening effect on the final  
20 mastics.



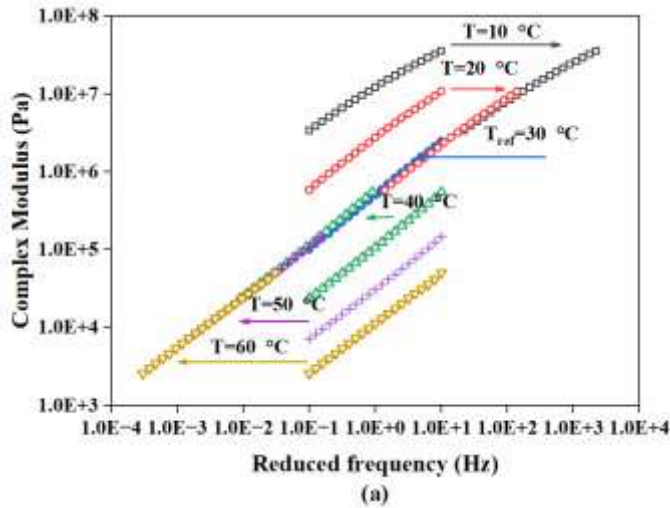
1  
2 **Figure 4. Black diagram of PmB and two mastic samples**

3 In this study, master curves were constructed employing a manual shift factor  
4 ( $\alpha_T$ ) that can be expressed as:

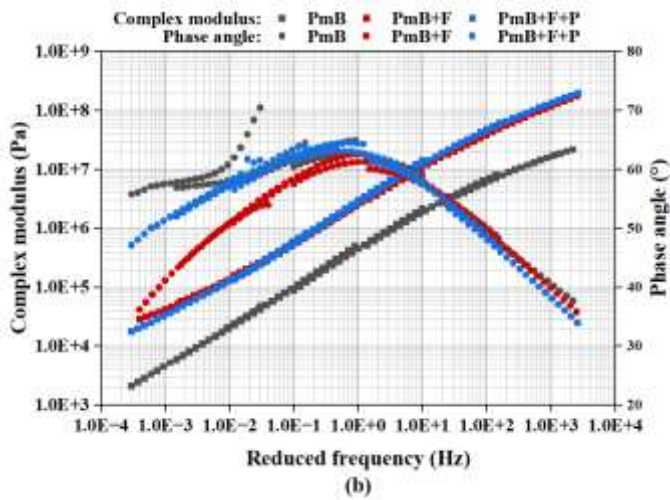
$$\alpha_T = \frac{f_r}{f} \quad (3)$$

5 where  $f$  is the raw frequency (from 0.1 Hz to 10 Hz) adopted in the FS tests, while  $f_r$   
6 means the reduced frequency at a reference temperature. Taking PmB as an example,  
7 Figure 5(a) displays how manual shift factors at six test temperatures were used to build  
8 complex modulus master curves at the reference temperature of 30 °C. Following the  
9 same procedures, master curves of the complex modulus and phase angle of the three  
10 samples are shown in Figure 5(b). As observed from the master curves of complex  
11 modulus, the curves of two mastic samples nearly overlapped with each other and both  
12 were almost parallel to the curve of PmB. Compared to the modified bitumen sample,  
13 complex modulus master curves of mastic samples showed an upward shift. This  
14 change illustrates that mastic samples had a higher stiffness due to the addition of fillers

1 confirming the penetration and softening point results. The different trend of phase  
2 angle master curves was also recorded in Figure 5(b). It can be found that the phase  
3 angles of tested samples increased and then decreased with the frequency increasing.  
4 No significant difference in phase angle values was found when the three samples were  
5 subjected to the higher frequencies (low temperatures). While, at low frequencies (high  
6 temperatures), distinctions among the three samples became more visible highlighting  
7 the different effects of filler quantity and type. PmB+F showed the lowest phase angle  
8 values, followed by PmB+F+P, then PmB. This implies that the addition of fillers  
9 improved the rutting resistance of modified bitumen, while introducing the powder  
10 caused a negative influence on the change in phase angle values.



1



2

3 **Figure 5. (a) Construction of the complex modulus master curves of PmB; (b) The complex**  
 4 **modulus and phase angle master curves of PmB and two mastics**

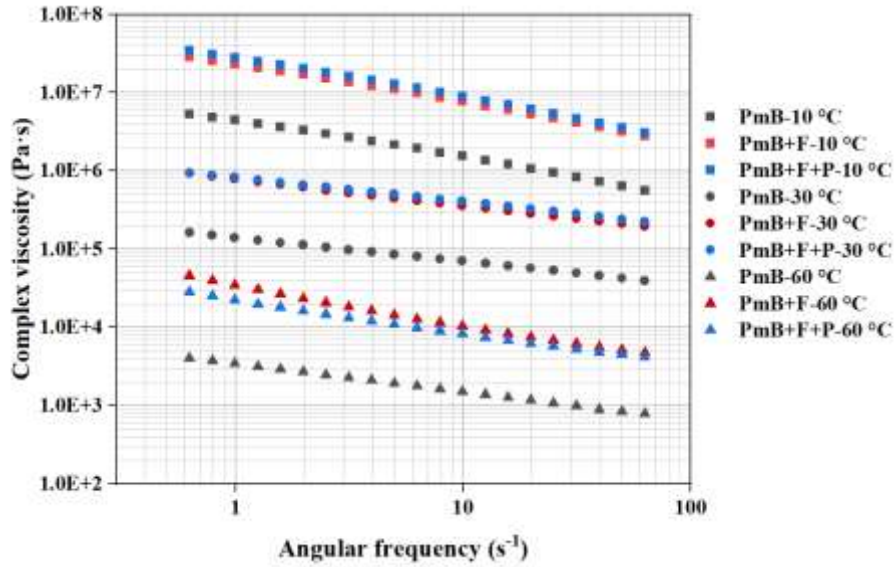
5 3.2.2.2 Complex viscosity and flow activation energy

6 According to the raw data collected from the FS tests, complex viscosity ( $\eta^*$ , Pa·s) can  
 7 be calculated by the following equation:

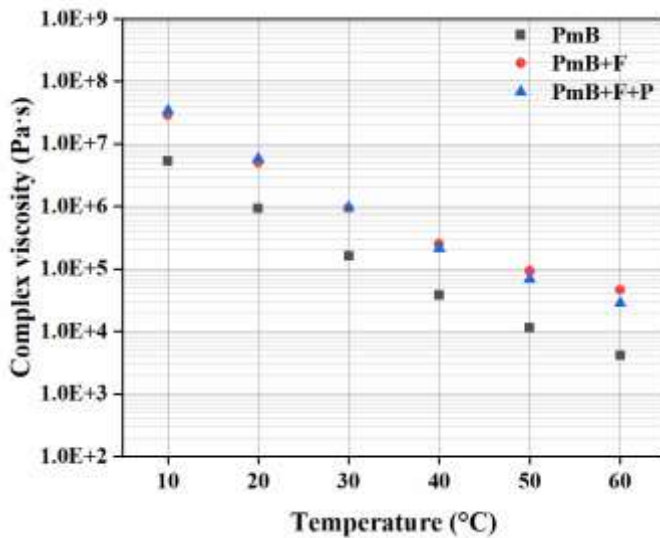
$$\eta^* = G^* / \omega \quad (4)$$

8 where  $G^*$  is the complex shear modulus (Pa) that was introduced before,  $\omega$  represents  
 9 the corresponding angular frequency (rad/s or  $s^{-1}$ ). Figure 6 presents the complex  
 10 viscosities of three testing samples at three temperatures (10°C, 30°C and 60°C). The

1 viscosity of bitumen or mastic is affected by the temperatures and frequencies. Samples  
2 subjected to the lowest temperature (10 °C) had the highest complex viscosity whereas  
3 the sample tested at 60 °C displayed the lowest  $\eta^*$ . PmB and the other two mastics all  
4 behaved like non-Newtonian fluids because viscosities showed an upward trend with  
5 the shear rate (angular frequency) decreasing. This behaviour reflects the basic  
6 rheological property of the tested bituminous binder and mastics, since the softening  
7 points of all materials are greater than 60 °C. Under the same temperature and frequency,  
8 both mastic samples displayed a higher  $\eta^*$  than PmB, meaning improved resistance to  
9 permanent deformation. This behaviour confirms the positive effect of filler particles  
10 on rutting phenomenon available in literature (Diab and Enieb 2018, Rochlani *et al.*  
11 2019). Comparing the two mastics, the influence of additional waste powder was  
12 clearer when tested at lower frequencies, hence at 60 °C. PmB+F+P had lower viscosity  
13 under this condition. For further investigation of the effect of additional powder,  
14 complex viscosity at the lowest angular frequency (0.63 rad/s) versus temperatures are  
15 plotted in Figure 7. With the increase in test temperatures, the incorporation of powder  
16 was unbeneficial to the deformation resistance.



1  
2 **Figure 6. Complex viscosity versus angular frequency of PmB and two mastics at 10°C, 30°C,**  
3 **and 60°C**

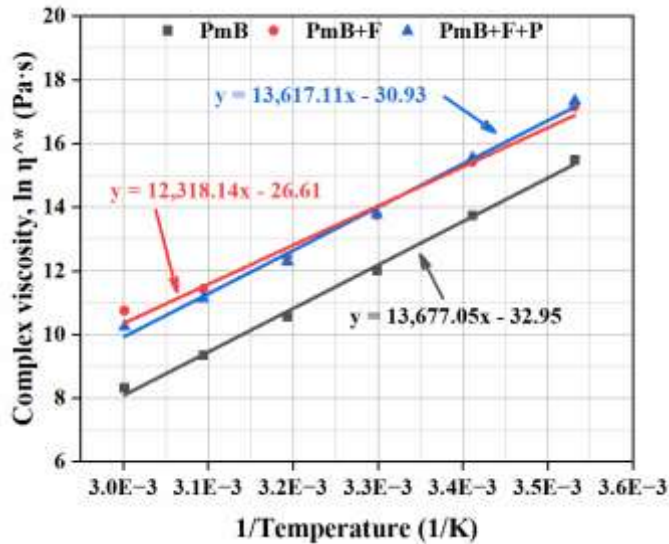


4  
5 **Figure 7. Complex viscosity versus temperatures at the lowest angular frequency (0.63 rad/s)**

6 The flow activation energy ( $E_a$ , KJ/mol) was used to evaluate the thermal  
7 susceptibility of modified bitumen and mastics.  $E_a$  can be obtained through the  
8 Arrhenius equation that is used to represent the temperature dependence of the viscosity  
9 of bitumen (Wang *et al.* 2018), which is shown below:

$$\eta^* = Ae^{E_a/RT} \quad (5)$$

1 where A is a pre-exponential parameter, R represents the universal gas constant (8.314  
 2 J/mol·K), then T is the testing temperature (K). In equation (3),  $\eta^*$  is the complex  
 3 viscosity at zero or low shear rate (Pa·s). The temperature dependence of  $\eta^*$  at the  
 4 lowest shear rate is depicted in Figure 8. The slopes of  $\ln\eta^*$  versus 1/Temperature curves  
 5 can be used to obtain the activation energy to flow. Table 10 lists the calculated results  
 6 of the flow activation energy. The results illustrate that the mastic with limestone filler  
 7 only showed the lowest activation energy. It reveals that the introduced filler reduced  
 8 the susceptibility of modified bitumen to the temperature variation, while the added  
 9 waste powder made the resulting mastic (PmB+F+P), more vulnerable to temperature  
 10 changes. In fact, the mastic sample containing filler and powder returned to the original  
 11 thermal susceptibility of PmB. The reason for this might be the organic residues in the  
 12 powder.



13  
 14 **Figure 8. Temperature dependence of  $\eta^*$  at the lowest shear rate**

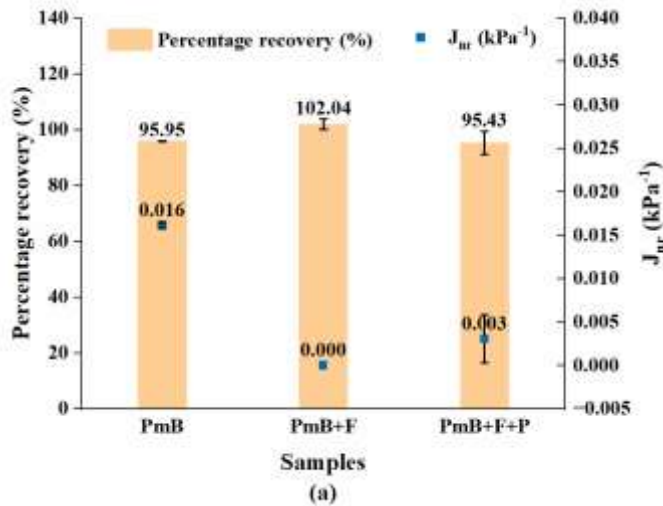
15  
 16

1 **Table 10. Flow activation energy for of PmB and two mastics**

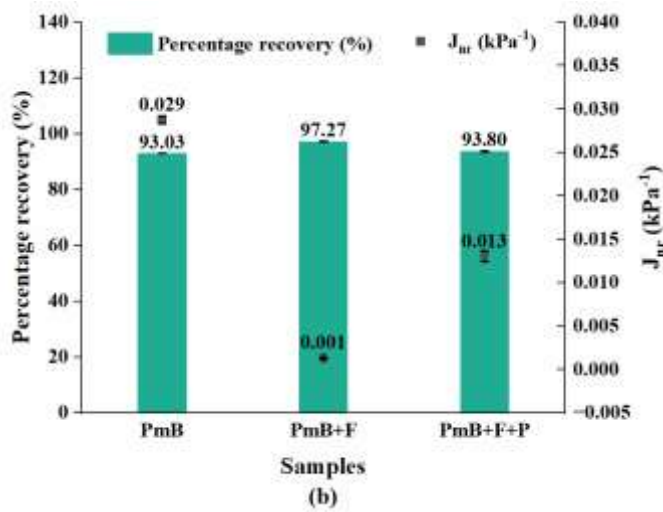
Sample	Flow activation energy ( $E_a$ , KJ/mol)
PmB	113.71
PmB+F	102.41
PmB+F+P	113.21

2 *3.2.3 Analysis of elastic behaviour from MSCR results*

3 According to MSCR tests, percentage recovery (R%) and non-recoverable creep  
 4 compliance ( $J_{nr}$ ) of the three samples tested at 0.1 kPa and 3.2 kPa were reported in  
 5 Figure 9 (a) and (b) respectively. With the stress level increasing, R% decreased while  
 6  $J_{nr}$  value increased. As depicted in Figure 9, mastic with only limestone filler had the  
 7 highest percentage recovery and the lowest  $J_{nr}$  value, indicating the highest rutting  
 8 resistance. This is because the addition of filler provides a good particle interaction with  
 9 bitumen, increasing the stiffness and improving the recovery response at high  
 10 temperature. However, the waste powders weakened this enhancement, as PmB+F+P  
 11 showed a lower percentage recovery and higher  $J_{nr}$  value compared to PmB+F. A  
 12 possible reason could be the softening effect of the organic components from the  
 13 powders at high temperature. This effect was more significant when comparing the  
 14 percentage recovery as R% values of mastic containing filler and powder were  
 15 extremely similar to the data of PmB. This means that the elastic behaviour of the mastic  
 16 containing only filler was nearly restored to the original level due to the addition of  
 17 powder. This result is in line with the flow activation energy discussed in the previous  
 18 section in which the similar thermal susceptibility of PmB and PmB+F+P was obtained.



1



2

3 **Figure 9. Percentage recovery (%) and  $J_{nr}$  at two stress levels: (a) 0.1 kPa; (b) 3.2 kPa**

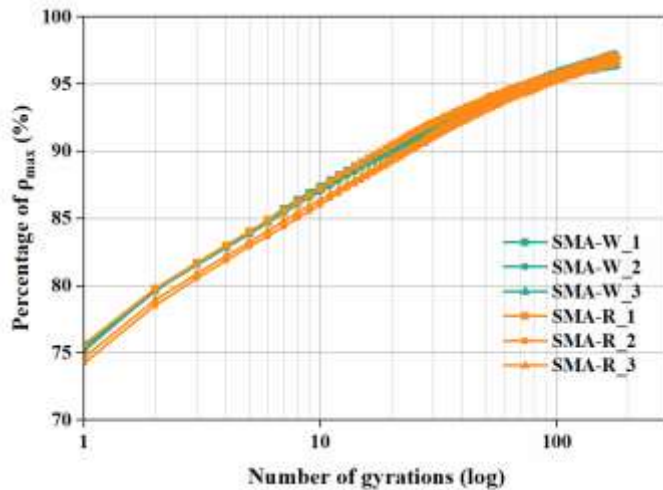
4 **3.3 Volumetric properties of SMA mixtures**

5 The compactability and workability of SMA mixtures were characterised using the AV  
 6 contents at 10, 100 and 180 gyrations. The results are reported in Table 11. A slightly  
 7 lower AV content was recorded for the SMA mixture using shredded E-CBs at 10  
 8 gyrations. With the compaction levels increasing, the two SMA mixtures achieved the  
 9 same value at 100 and 180 gyrations, whose AV contents were lower than 5% and met  
 10 the requirements of the technical specification used as reference. Besides, gyratory  
 11 compaction curves of the two types of SMA mixtures (three samples for each type) are

1 plotted in Figure 10. It can be observed that no significant changes were found among  
 2 all tested SGC samples in terms of maximum densification ( $\rho_{\max}$ ). Therefore, the results  
 3 of AV content and gyratory compaction curves indicate that both SMA mixtures showed  
 4 comparable physical properties; no unfavourable effect of using shredded E-CBs as  
 5 fibres was found on the volumetric properties of the SMA mixture.

6 **Table 11. AV contents of SGC samples at 10, 100 and 180 gyrations**

Samples	AV (%) at 10 gyrations	AV (%) at 100 gyrations	AV (%) at 180 gyrations
SMA-W	12.8 ( $\pm 0.2$ )	4.4 ( $\pm 0.2$ )	3.2 ( $\pm 0.4$ )
SMA-R	13.4 ( $\pm 0.6$ )	4.4 ( $\pm 0.2$ )	3.2 ( $\pm 0.3$ )



7  
 8 **Figure 10. Gyratory compaction curves of SMA samples**

9 **3.4 Mechanical properties of SMA samples**

10 **3.4.1 ITS results**

11 The ITS test is an effective method to evaluate the cohesion property of asphalt mixtures,  
 12 i.e., the bonding ability of bitumen-filler-aggregates (Sangiorgi *et al.* 2014). Six SGC  
 13 specimens (three for SMA-W and three for SMA-R) were kept in a temperature-  
 14 controlled chamber for a minimum of four hours and then tested at 25 °C. The average  
 15 results of the two mixes are presented in Table 12. SMA-R had a higher ITS value

1 compared to SMA-W, indicating the increasing cohesion of this mixture. However, it  
 2 should be noted that the ITS results for the two SMA mixes were both higher than 0.90  
 3 MPa, meeting the threshold limit required in the technical standard used as reference.  
 4 Besides, the lower displacement of SMA-R was also in accordance with its higher  
 5 stiffness, as verified in the following mechanical dynamic analysis.

6 **Table 12. ITS of two SMA samples at 25 °C**

SMA sample	Thickness (mm)	Max load (N)	Displacement (mm)	ITS (MPa)	Avg. ITS (MPa)
SMA-W	1	53.0	9850	2.94	1.18
	2	53.2	10770	3.12	1.29
	3	52.9	10550	3.20	1.27
SMA-R	1	51.6	11690	2.44	1.44
	2	51.9	11700	2.78	1.43
	3	51.9	10890	2.60	1.34

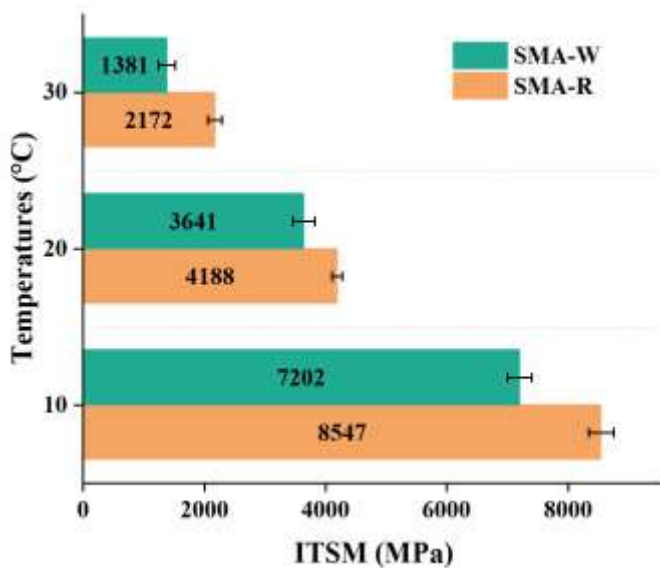
7 *3.4.2 ITSM results*

8 The stiffness modulus results of the two SMA mixtures at three different test  
 9 temperatures are presented in Figure 11. Compared to the referenced samples, a  
 10 reduction in stiffness modulus at each temperature was recorded for SMA mix  
 11 containing shredded E-CBs. Besides, both samples satisfied the technical specification  
 12 used as reference, in which the ITSM value at 20 °C is required to be above 3500 MPa.  
 13 The thermal susceptibility can be evaluated with the ITSM versus temperature curve  
 14 described by the equation below:

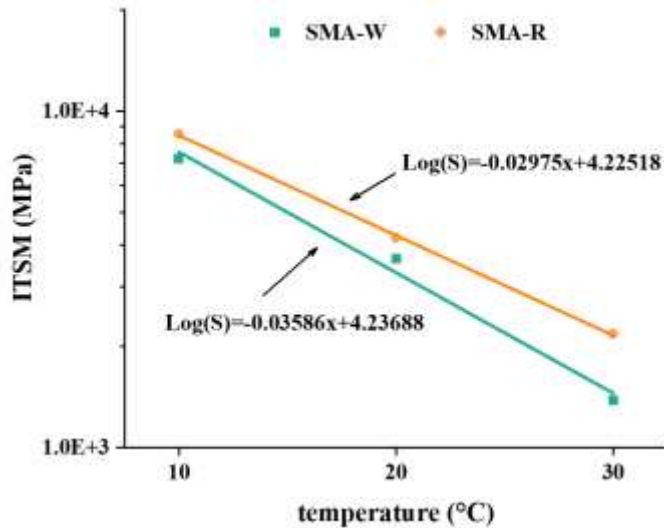
$$\log S = -\alpha \cdot T + \beta \quad (6)$$

15 where S is the indirect tensile stiffness modulus (ITSM) at the testing temperature T,  
 16 then  $\alpha$  and  $\beta$  are experimental parameters relevant to the properties of materials. Among

1 these parameters,  $\alpha$  can be used to represent the temperature susceptibility. The ITSM  
2 versus temperature curves of SMA-W and SMA-R and the corresponding equations are  
3 shown in Figure 12. It can be seen that  $\alpha$  parameter for SMA-W and SMA-R are  
4 0.03586 and 0.02975 respectively. A higher  $\alpha$  parameter implies that the material is  
5 more sensitive to temperature changes. By comparison, the results from this dynamic  
6 mechanical test show that using the shredded E-CBs to replace traditional cellulose  
7 fibres in SMA resulted in a slight increase in this parameter, but the modification effect  
8 on thermal susceptibility was not remarkable.



9  
10 **Figure 11. ITSM results of two SMA samples**



1  
2 **Figure 12. ITSM average results versus temperature**

3 *3.4.3 ITSR results*

4 Moisture damage, as one of the major distresses in asphalt pavements, is caused by the  
5 reduction in the adhesive bond between bitumen and aggregates. The presence of water  
6 is mainly responsible for the loss of adhesion ability. To assess the moisture  
7 susceptibility of the two SMA mixtures, six SGC specimens were immersed in the 40 °C  
8 water for 72 hours before following the procedures performed for the ITS test. The ITS  
9 values of each specimen after the water bath are given in Table 13 ( $ITS_{wet}$ ).

10 The ITSR values were calculated subsequently and listed in Table 14 as the  
11 results of the ratio between ITS data obtained on samples after normal ( $ITS_{dry}$ ) or wet  
12 conditioning ( $ITS_{wet}$ ). It can be clearly seen that two SMA mixtures have extremely  
13 higher ITSR values, showing a low water susceptibility. As required by the technical  
14 standard, both mixtures met the minimum level of ITSR value (75%). It should be noted  
15 that the ITSR of SMA-W is above 100%. Therefore, the use of shredded E-CBs might  
16 represent a potential improvement for the asphalt concrete against moisture damage.

1 **Table 13. ITS<sub>wet</sub> of two SMA samples after a water bath at 40 °C for 72 hours**

SMA sample	Thickness (mm)	Max load (N)	Displacement (mm)	ITS <sub>wet</sub> (MPa)	Avg. ITS <sub>wet</sub> (MPa)
SMA-W	1	53.4	10320	2.86	1.23
	2	54.2	11060	3.06	1.30
	3	53.1	11530	2.66	1.38
SMA-R	1	52.8	10870	2.78	1.31
	2	52.4	10280	2.94	1.25
	3	52.0	11670	2.76	1.43

2 **Table 14. ITSR results of two SMA samples**

SMA sample	ITS <sub>dry</sub> (MPa)	ITS <sub>wet</sub> (MPa)	ITSR (%)
SMA-W	1.25	1.30	105
SMA-R	1.40	1.33	95

3 *3.4.4 RLAT analysis*

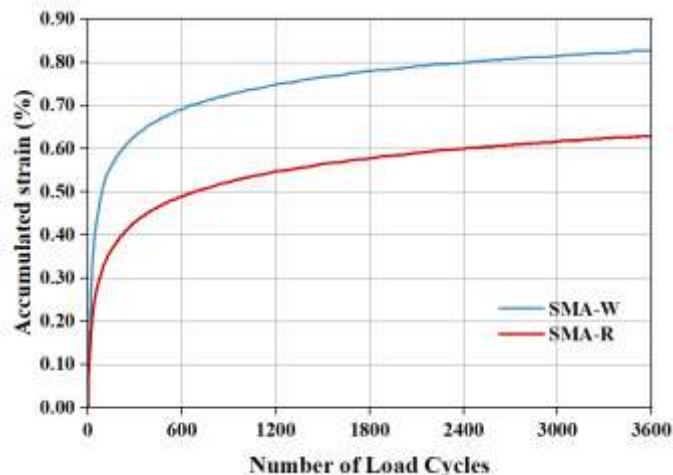
4 The RLAT performed using a uniaxial compression configuration is considered an  
5 effective method of evaluating the specimen's resistance to permanent deformation  
6 under dynamic loading and elevated temperature. In this test, the specimen was placed  
7 between two parallel plates, where the upper plate has a smaller diameter compared to  
8 the asphalt specimen. Then the specimen was subjected to a periodic loading with a  
9 frequency of 0.5 Hz and a stress of 100±2 kPa. After 3600 loading cycles that lasted  
10 around 2 hours at the temperature of 40 °C, the accumulated axial deformation was  
11 subsequently recorded. The accumulated strain and creep stiffness collected from  
12 RLAT were used to compare the potential rutting resistance of SMA mixtures with two  
13 different fibres. Their average results are listed in Table 15. Besides, Figure 13 presents  
14 the development of accumulated strain with the number of load cycles.

15

16

1 **Table 15. Accumulated strain and creep modulus from RLAT tests**

SMA sample	Accumulated strain (%)	Creep stiffness (MPa)
SMA-W	0.83 ( $\pm 0.01$ )	12.1 ( $\pm 0.05$ )
SMA-R	0.63 ( $\pm 0.01$ )	15.9 ( $\pm 0.36$ )



2

3 **Figure 13. The curves of accumulated strain versus number of load cycles**

4 It is visible that the presence of shredded E-CBs in SMA resulted in a higher  
5 accumulated strain and lower creep stiffness compared to the reference, implying  
6 decreased resistance to permanent deformation. From the analysis of the curves in  
7 Figure 13, two stages can be detected: the initial stage of deformation, in which a rapid  
8 increase in accumulated strain is recorded; and the second stage where the slope of the  
9 curve is quasi constant until the end of the test. The two mixtures showed a similar  
10 behaviour, considering that the end of the initial stage was verified at around 400 cycles  
11 for both SMA. However, the accumulated strain rate was higher for the mixture with  
12 E-CBs, indicating the lower rutting resistance of the mixture. This result is in line with  
13 the higher mechanical properties verified for the reference SMA. Unlike the creep  
14 stiffness values of SMAs with PmB and fibres above 25 MPa (Eskandarsefat *et al.* 2019,  
15 Tataranni and Sangiorgi 2021), the results in this research were lower, which can be

1 explained by the different rheological changes brought about by the addition of bitumen.  
2 Additionally, the modification to the rheological property caused by the presence of  
3 waste powder had a different impact on the mechanical properties of asphalt mixtures  
4 in this study. The same comparison results also can be found in ITSM tests where lower  
5 ITSM values of this research were recorded.

#### 6 **4 Conclusions**

7 In the presented research, the possibility of using waste electronic cigarette butts (E-  
8 CBs) in SMA mixtures as a replacement of traditional cellulose stabilising fibres was  
9 investigated. Based on the collected experimental data, the main conclusions are  
10 summarised below:

- 11 ● According to the drain-down tests, samples with 0.3% or 0.4% shredded E-CBs  
12 showed suitable bitumen absorption properties, comparable with cellulose fibres  
13 used as a stabilising agent for high bitumen content asphalt concretes.
- 14 ● Based on the penetration and softening point results, the mastic with limestone  
15 filler was stiffer than the mastic containing filler and waste powder. The addition  
16 of powders led to the significant decrease in the softening point.
- 17 ● According to FS tests, both mastics displayed similar complex modulus, while  
18 PmB+F showed lower phase angle values at low frequencies (high temperatures).  
19 It means that adding the powder is detrimental to the elastic behaviour of  
20 bituminous materials. The gap between the complex viscosity of the two mastics  
21 also became larger at lower frequencies with the increasing temperature. The

1 comparison of flow activation energy confirmed these results, the mastic  
2 containing fillers and powders showed a higher thermal susceptibility than the  
3 mastic without the waste powder. The negative effect on the thermal susceptibility  
4 might be related to the presence of organic ashes.

5 ● Two critical parameters from MSCR tests,  $R\%$  and  $J_{nr}$ , demonstrate that the mastic  
6 with filler had better rutting resistance than the mastic containing filler and waste  
7 powder. It should be noted that powder is responsible for the loss of  $R\%$ ,  
8 unfavourable to the elastic behaviour.

9 ● In terms of the volumetric properties, SMA mixes with the two different fibres  
10 achieved excellent workability and compactability, showing nearly the same air  
11 void content. Thus, the addition of shredded E-CBs did not modify the workability  
12 properties of the SMA.

13 ● Based on mechanical test results, the decrease in stiffness modulus and cohesion  
14 property were recorded for SMA-W samples compared to the reference (SMA-R).  
15 The use of shredded E-CBs also led to a higher thermal susceptibility and a lower  
16 water susceptibility, but the effect was not significant. By means of RLAT, it was  
17 proved that SMA with shredded E-CBs had lower resistance to permanent  
18 deformation than the reference, confirming also the rheological results.

19 Overall, SMA-W mix meets the technical requirements for this type of asphalt  
20 concrete based on the tested results, though the experimental analysis on bituminous  
21 mastics and mixtures highlighted the detrimental effects of E-CBs components on the

1 rheo-mechanical behaviour of the final product. These effects may be ascribed to the  
2 plastic particles and other powders coming from the shredding process of waste  
3 cigarette filters. Future studies will try to optimise the treatment of waste E-CBs, aiming  
4 to improve the mechanical properties of asphalt mixtures by replacing cellulose fibres  
5 and promoting the recycling of cigarette butts.

#### 6 **Declaration of Competing Interest**

7 The authors declare that they have no known competing financial interests or personal  
8 relationships that could have appeared to influence the work reported in this paper.

#### 9 **Acknowledgments**

10 The first author would like to gratefully acknowledge the funding support from China  
11 Scholarship Council (CSC) under the grant CSC No. 202106150028.

#### 12 **References**

- 13 AASHTO T305, 2012, Standard method of test for determination of draindown  
14 characteristics in uncompacted asphalt mixtures. Washington, DC: American  
15 Association of State and Highway Transportation Officials.
- 16 Airey, G.D., 2002. Use of black diagrams to identify inconsistencies in rheological data.  
17 *Road Materials and Pavement Design*, 3 (4), 403–424.
- 18 Ariza, E., Jiménez, J.A., and Sardá, R., 2008. Seasonal evolution of beach waste and  
19 litter during the bathing season on the Catalan coast. *Waste Management*, 28 (12),  
20 2604–2613.

- 1 ASTM D6390—11, 2017. Standard Test Method for Determination of Draindown  
2 Characteristics in Uncompacted Asphalt Mixtures. ASTM International.
- 3 ASTM D7405, 2015. Standard Test Method for Multiple Stress Creep and Recovery  
4 (MSCR) of Asphalt Binder Using a Dynamic Shear Rheometer. ASTM  
5 International.
- 6 Brown, E., Mallick, R.B., Haddock, J.E., and Bukowski, J., 1997. *Performance of stone*  
7 *matrix asphalt (SMA) mixtures in the United States*. National Center for Asphalt  
8 Technology.
- 9 Capitolato Speciale d'Appalto. Comune di Bologna. Capo III—Opere Stradali. 2018.
- 10 Cardoso, L.S., Estrela, F.N., Chagas, T.Q., da Silva, W.A.M., Costa, D.R. de O., Pereira,  
11 I., Vaz, B.G., Rodrigues, A.S. de L., and Malafaia, G., 2018. The exposure to water  
12 with cigarette residue changes the anti-predator response in female Swiss albino  
13 mice. *Environmental Science and Pollution Research*, 25 (9), 8592–8607.
- 14 Compa, M., Ventero, A., Iglesias, M., and Deudero, S., 2018. Ingestion of microplastics  
15 and natural fibres in *Sardina pilchardus* (Walbaum, 1792) and *Engraulis*  
16 *encrasicolus* (Linnaeus, 1758) along the Spanish Mediterranean coast. *Marine*  
17 *Pollution Bulletin*, 128, 89–96.
- 18 Conradi, M. and Sánchez-Moyano, J.E., 2022. Toward a sustainable circular economy  
19 for cigarette butts, the most common waste worldwide on the coast. *Science of the*  
20 *Total Environment*, 847, 157634.
- 21 Cullen, K.A., Gentzke, A.S., Sawdey, M.D., Chang, J.T., Anic, G.M., Wang, T.W.,

- 1 Creamer, M.R., Jamal, A., Ambrose, B.K., and King, B.A., 2019. e-Cigarette Use  
2 Among Youth in the United States, 2019. *JAMA*, 322 (21), 2095–2103.
- 3 Diab, A. and Enieb, M., 2018. Investigating influence of mineral filler at asphalt  
4 mixture and mastic scales. *International Journal of Pavement Research and*  
5 *Technology*, 11 (3), 213–224.
- 6 Dobaradaran, S., Mutke, X.A.M., Schmidt, T.C., Swiderski, P., De-la-Torre, G.E., and  
7 Jochmann, M.A., 2022. Aromatic amines contents of cigarette butts: fresh and  
8 aged cigarette butts vs unsmoked cigarette. *Chemosphere*, 301, 134735.
- 9 Dobaradaran, S., Soleimani, F., Akhbarizadeh, R., Schmidt, T.C., Marzban, M., and  
10 BasirianJahromi, R., 2021. Environmental fate of cigarette butts and their toxicity  
11 in aquatic organisms: A comprehensive systematic review. *Environmental*  
12 *Research*, 195, 110881.
- 13 EN 1426: 2015. Bitumen and bituminous binders. Determination of needle penetration.  
14 European standard.
- 15 EN 1427: 2015. Bitumen and bituminous binders. Determination of the softening point.  
16 Ring and Ball method. European standard.
- 17 EN 12697-12: 2018. Bituminous mixtures. Test methods. Determination of the water  
18 sensitivity of bituminous specimens. European standard.
- 19 EN 12697-23: 2017. Bituminous mixtures. Test methods. Determination of the indirect  
20 tensile strength of bituminous specimens. European standard.
- 21 EN 12697-25: 2020. Bituminous mixtures. Test methods. Cyclic compression test.

- 1 European standard.
- 2 EN 12697-26: 2018. Bituminous mixtures. Test methods. Stiffness. European standard.
- 3 EN 12697-31: 2019. Bituminous mixtures. Test methods. Specimen preparation by  
4 gyratory compactor. European standard.
- 5 EN 13398: 2017. Bitumen and bituminous binders. Determination of the elastic  
6 recovery of modified bitumen. European standard.
- 7 EN 13399: 2017. Bitumen and bituminous binders. Determination of storage stability  
8 of modified bitumen. European standard.
- 9 EN 13702-1: 2003. Bitumen and bituminous binders. Determination of dynamic  
10 viscosity of modified bitumen. Cone and plate method. European standard.
- 11 EN 14770: 2012. Bitumen and bituminous binders. Determination of complex shear  
12 modulus and phase angle. Dynamic Shear Rheometer (DSR). European standard.
- 13 Eskandarsefat, S., Dondi, G., and Sangiorgi, C., 2019. Recycled and rubberized SMA  
14 modified mixtures: A comparison between polymer modified bitumen and  
15 modified fibres. *Construction and Building Materials*, 202, 681–691.
- 16 Eurobarometer, S., 2015. Attitudes of Europeans towards tobacco and electronic  
17 cigarettes. *TNS Opinion Social*, 429, 1-142.
- 18 Gerritse, J., Leslie, H.A., de Tender, C.A., Devriese, L.I., and Vethaak, A.D., 2020.  
19 Fragmentation of plastic objects in a laboratory seawater microcosm. *Scientific  
20 Reports*, 10 (1), 10945.
- 21 Giovacchini, C.X., Crotty Alexander, L.E., and Que, L.G., 2022. Electronic Cigarettes:

- 1 A Pro–Con Review of the Current Literature. *The Journal of Allergy and Clinical*  
2 *Immunology: In Practice*, 10 (11), 2843–2851.
- 3 Hidalgo-Ruz, V., Honorato-Zimmer, D., Gatta-Rosemary, M., Nuñez, P., Hinojosa, I.A.,  
4 and Thiel, M., 2018. Spatio-temporal variation of anthropogenic marine debris on  
5 Chilean beaches. *Marine Pollution Bulletin*, 126, 516–524.
- 6 Mohajerani, A., Kadir, A.A., and Larobina, L., 2016. A practical proposal for solving  
7 the world’s cigarette butt problem: Recycling in fired clay bricks. *Waste*  
8 *Management*, 52, 228–244.
- 9 Mohajerani, A., Tanriverdi, Y., Nguyen, B.T., Wong, K.K., Dissanayake, H.N., Johnson,  
10 L., Whitfield, D., Thomson, G., Alqattan, E., and Rezaei, A., 2017. Physico-  
11 mechanical properties of asphalt concrete incorporated with encapsulated cigarette  
12 butts. *Construction and Building Materials*, 153, 69–80.
- 13 Ocean Conservancy, 2021. Ocean conservation. Pandemic pollution: the rising tide of  
14 plastic PPE.
- 15 Rahman, M.T. and Mohajerani, A., 2020. Use of bitumen encapsulated cigarette butts  
16 in stone mastic asphalt. *Construction and Building Materials*, 261, 120530.
- 17 Rahman, M.T., Mohajerani, A., and Giustozzi, F., 2020a. Recycling of waste materials  
18 for asphalt concrete and bitumen: A review. *Materials*, 13 (7), 1495.
- 19 Rahman, M.T., Mohajerani, A., and Giustozzi, F., 2020b. Possible recycling of cigarette  
20 butts as fiber modifier in bitumen for asphalt concrete. *Materials*, 13 (3), 734.
- 21 Rochlani, M., Leischner, S., Falla, G.C., Wang, D., Caro, S., and Wellner, F., 2019.

1 Influence of filler properties on the rheological, cryogenic, fatigue and rutting  
2 performance of mastics. *Construction and Building Materials*, 227, 116974.

3 Roder Green, A.L., Putschew, A., and Nehls, T., 2014. Littered cigarette butts as a  
4 source of nicotine in urban waters. *Journal of Hydrology*, 519, 3466–3474.

5 Sangiorgi, C., Tataranni, P., Simone, A., Vignali, V., Lantieri, C., and Dondi, G., 2014.  
6 Waste bleaching clays as fillers in hot bituminous mixtures. *Construction and*  
7 *Building Materials*, 73, 320–325.

8 Soleimani, F., Dobaradaran, S., De-la-Torre, G.E., Schmidt, T.C., and Saeedi, R., 2022.  
9 Content of toxic components of cigarette, cigarette smoke vs cigarette butts: A  
10 comprehensive systematic review. *Science of The Total Environment*, 813, 152667.

11 Tataranni, P. and Sangiorgi, C., 2021. A preliminary laboratory evaluation on the use of  
12 shredded cigarette filters as stabilizing fibers for stone mastic asphalts. *Applied*  
13 *Sciences (Switzerland)*, 11 (12), 5674.

14 Vázquez, V.F., Terán, F., Luong, J., and Paje, S.E., 2019. Functional Performance of  
15 Stone Mastic Asphalt Pavements in Spain: Acoustic Assessment. *Coatings*, 9 (2),  
16 123.

17 Victory, W., 2022. A review on the utilization of waste material in asphalt pavements.  
18 *Environmental Science and Pollution Research*, 29 (18), 27279–27282.

19 Wang, H., Liu, X., Apostolidis, P., and Scarpas, T., 2018. Rheological behavior and its  
20 chemical interpretation of crumb rubber modified asphalt containing warm-mix  
21 additives. *Transportation Research Record*, 2672 (28), 337–348.

- 1 Willis, J.R. and Yin, F., 2022. "Road-grade" recycled plastics: A critical discussion.
- 2 *Plastic Waste for Sustainable Asphalt Roads*, 43–59.
- 3